Supporting Information

Virtual loudspeaker effect of graphene-based hybrid material to improve low frequency acoustic performance

Ji Hoon Kim[2, ‡], Sun Taek Lim[2, ‡], Gyu Hyeon Shim[2], Gil Won Lee[2], Sungjoo Kim[3], Namkeun Kim[2], Somchai Wongwises[4] and Ho Seon Ahn[, 1, 2]*

[1]Division of Thermal and Fluids Science, Institute for computational Science; Faculty of Electrical and Electronics Engineering, Ton Duc Thang University, Ho Chi Minh City, Vietnam.

[2]Department of Mechanical Engineering, Incheon National University, Academy-ro, Yeonsu-gu, Incheon, 22012, Republic of Korea.

[3]SAMSUNG Electronics Co. Ltd., Samsung-ro, Yeongtong-gu, Suwon-si, Gyenggi-do, Republic of Korea.

[4]Department of Mechanical Engineering, King Mongkut's University of Technology Thonburi, Bangkok, Thailand.

‡These authors contribute equally.

[*]Corresponding author: hsahn@tdtu.edu.vn, hsahn@inu.ac.kr

1. Preparation of acoustic filling materials

1.1. Synthesis of thermally expanded graphene oxide powder

To synthesize the TEGO powder, we first fabricated GO using the modified Hummers' method[1]. There are three processes: (i) oxidation, (ii) rinsing, and (iii) freeze drying. As a first step, oxidation, graphite powder (2 g, flake type; Alfa Aesar) and $NaNO_3$ (1 g, ≥ 99.0 %; Sigma-Aldrich) were added to H_2SO_4 (69 ml, 95 %; Daejung) and we stirred them while maintaining the temperature below 10 ℃ using an ice bath. $KMnO_4$ (6 g, ≥ 99.0 %; Sigma-Aldrich) was dropped into a reaction flask for 10 minutes and reacted carefully for 7 hours, so that the temperature of the mixture did not exceed 20 ℃. The mixture was stirred for 2 hours as the temperature was maintained at 35 ℃. We then added the solution, which was mixed with deionized water (400 ml) and H_2O_2 (3 ml, 30%; Daejung), using a biuret and maintained the temperature of the mixture below 10 ℃. Then, a GO cake was obtained by vacuum filtering the sludge obtained from the previous process. The second process, i.e., rinsing, was carried out in two steps: rinsing the GO cake with deionized water (500 ml), and rinsing the GO cake with a mixed solution of HCl (300 ml, 35.0~37.0%; Samchun) and deionized water (300 ml). We carried out centrifugation (Fleta 40; Hanil) for 30 min at 4,000 ppm at the end of the process. To remove the remaining impurities, such as $KMnO_4$, from the GO cake, we alternated between rinsing with deionized water then mixing the solution. Then, the GO cake was rinsed five times, using deionized water to decrease its pH, and freeze dried for 4 days. Finally, we obtained GO powder that was bright-brown in color by crumbling a lump of GO into a bowl. The GO powders were carefully contained by an alumina boat and thermally treated under 0.5 L min-1 of Ar atmosphere at target annealing temperatures from 100 to 600 ℃.

1.2. Commercial materials

The commercial AC powder (Mendota), GP750 (xGnP® graphene nanoplatelets; Sigma-Aldrich) and MF were purchased commercially.

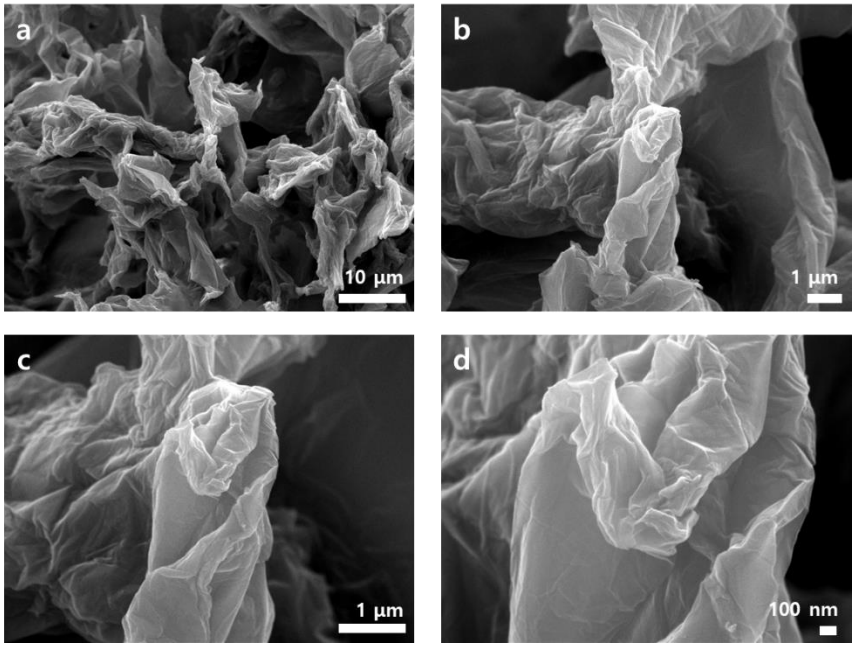

Figure S1. Scanning electron microscopy (SEM) image of as-prepared graphite oxide (GO) powders at various magnifications (a–d).

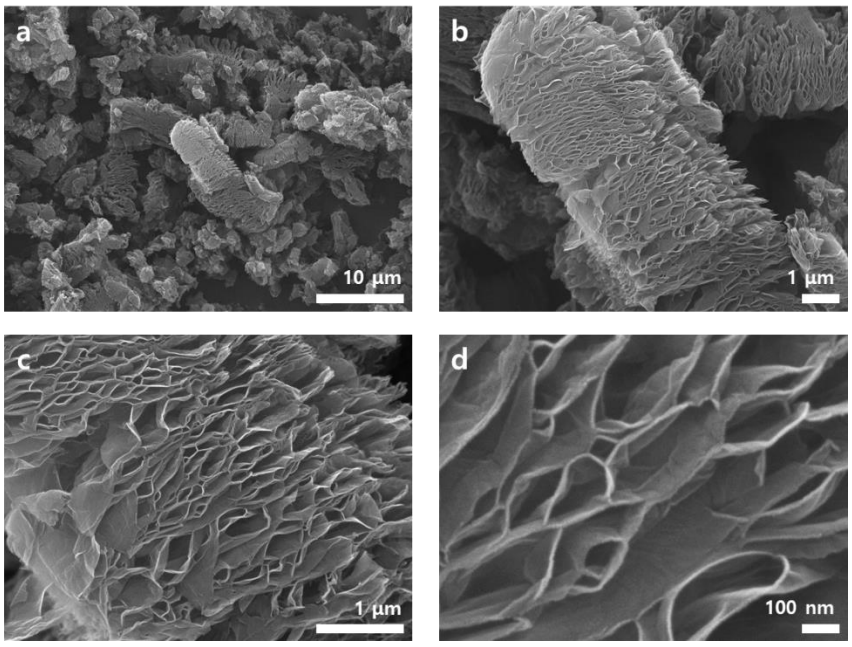

Figure S2. SEM image of thermally expanded graphene oxide (TEGO) powders at different magnifications (a–d).

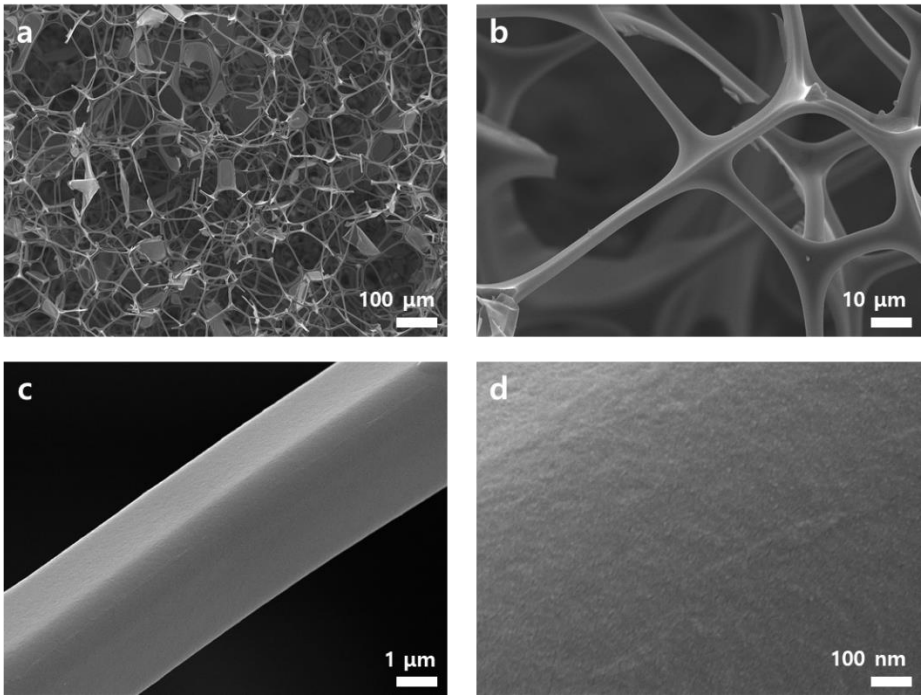

Figure S3. SEM image of melamine foam (MF) at different magnifications (a–d).

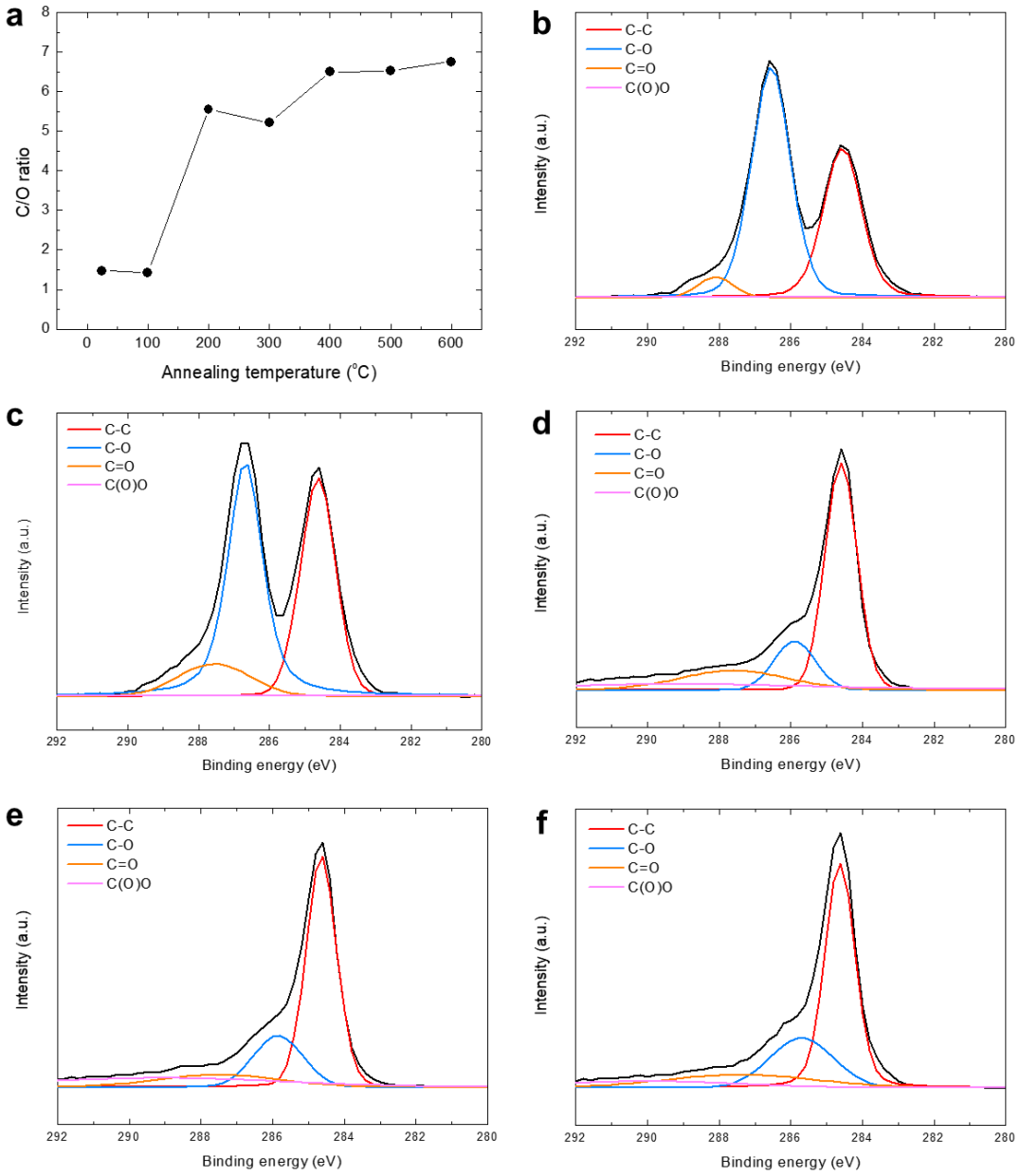

Figure S4. X-ray photoelectron spectroscopy (XPS) spectra. (a) C/O ratio of TEGO with respect to annealing temperature. C1s XPS spectra of (b) GO, (c) TEGO at 100 ℃, (d) TEGO at 200 ℃, (e) TEGO at 400 ℃, and (f) TEGO at 600 ℃.

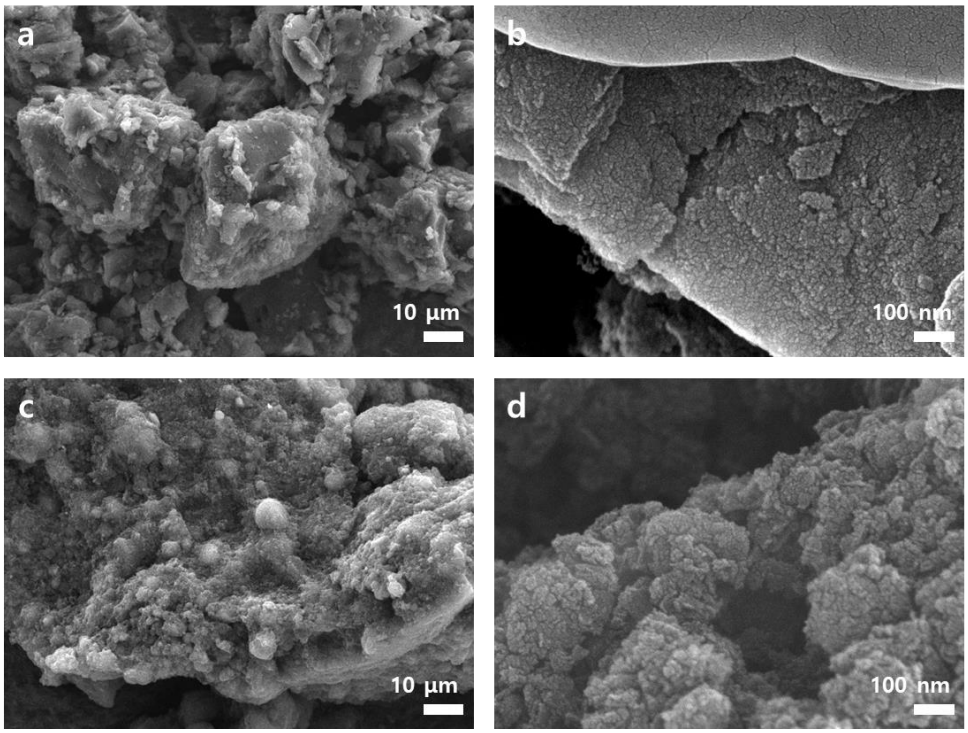

Figure S5. SEM image of commercial adsorptive materials. (a, b) Activated carbon (AC) with different magnifications. (c, d) GP750 with different magnifications.

2. Acoustic analysis: theory and procedures

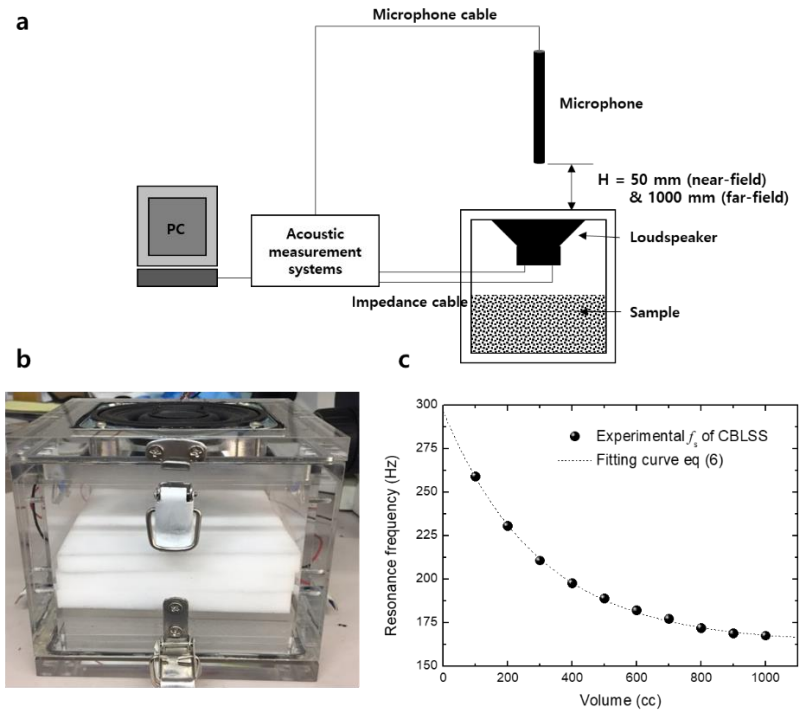

Figure S6. Acoustic measurement system. (a) Schematic diagram of the acoustic measurement system, which consists of a closed-box loudspeaker system (CBLSS), acoustic analyzer, acoustic filling material and microphone. (b) Digital image of acrylic CBLSS test section. (c) Resonance frequency of CBLSS with respect to volume, and fitting curve.

Figure S6a illustrates the setup of the CBLSS and acoustic analyzer. Acrylic CBLSSs (10 × 10 × 10 cm^3) were prepared so that we could measure their acoustic performances (Figure S3b). For convenience, the enclosure was formed by combining a main chamber, bottom cover, and top cover and the three parts were combined with an O-ring seal. The interior volume of the enclosure can be adjusted from 100 cc to 1,000 cc by adding 100 cc of acrylic plates to the main chamber. The samples were located in the cavity formed between the cover and the main chamber. The

round, 8-inch LS was fixed to the top cover of the enclosure and the nominal impedance of the voice coil was 3 Ohm. We measured the response of the electrical impedance with a sweeping signal, the frequency of which varied from 20 to 20,000 Hz within 3 seconds, under a potential of 1.23 V. For the measurement, we generated the signal using an acoustic analyzer (CLIO Pocket; Audiomatica; 1 Hz to 45 kHz, 0.01 Hz of resolution), which was connected to the LS voice-coil by a serial connection. To measure the SPL, a microphone was located 50 mm (near-field) and 1,000 mm (far-field) from the LS and connected to the acoustic analyzer. The SPL was measured in the same manner as the impedance, with frequencies from 20 to 20,000 Hz, using a sweeping signal.

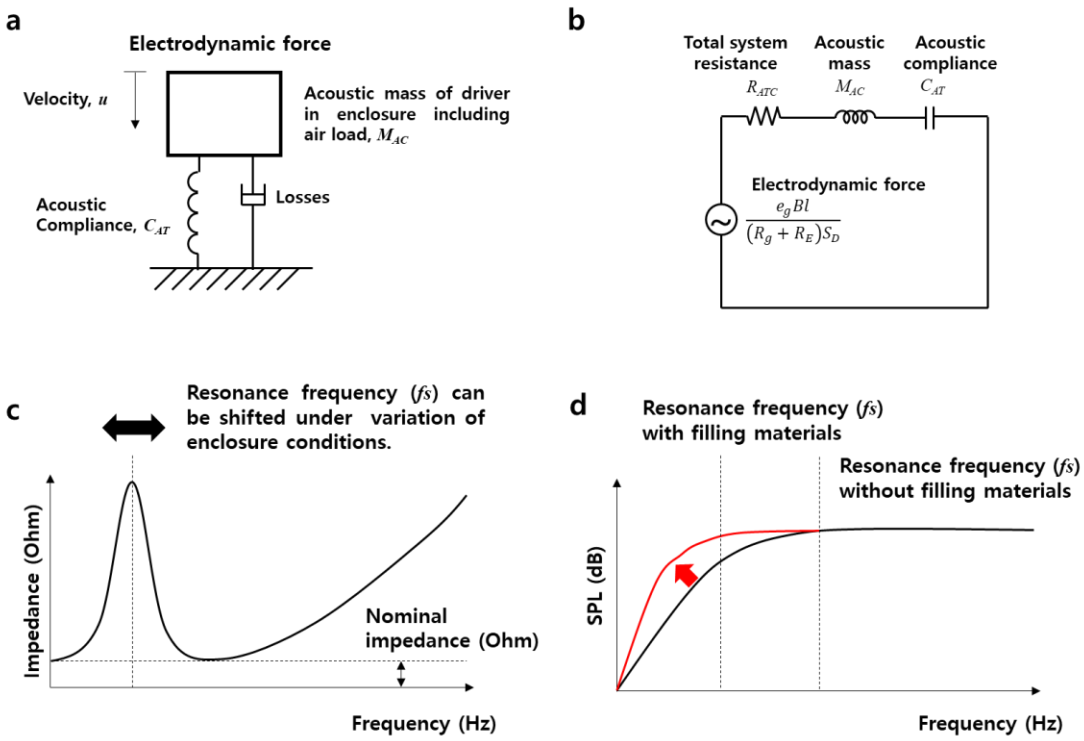

Figure S7. Acoustic model of the CBLSS. **(**a) Simplified vibrational model of the LS driver. (b) Simplified acoustical analogous circuit of CBLSS[2]. (c) Typical impedance curve of CBLSS. (d) Typical sound pressure level (SPL) curve of CBLSS.

For the CBLSS, the acoustic volume velocity is caused entirely by the motion of the LS driver (Figure S7a). According to the acoustic analogy, each component that governs the piston-like motion of the LS driver can be represented as an electrical equivalent circuit (Figure S7b). The volume of the air inside the enclosure, V_{AS}, acts as a suspension. In the equivalent circuit, the acoustic compliance of the closed-box loudspeaker system C_{AT} (or air-suspension loudspeaker system) appears as series of the suspension compliance C_{AS} and the compliance of the box C_{AB}[3].

$$C_{AT} = \left[\frac{1}{C_{AS}} + \frac{1}{C_{AB}} \right]^{-1} = \frac{C_{AS} C_{AB}}{C_{AS} + C_{AB}} \tag{1}$$

In case of the CBLSS, the suspension compliance C_{AS} are made very large, the compliance of the box C_{AB} could be made much smaller ($C_{AS} \gg C_{AB}$).

Thus, the equation (1) yields,

$$C_{AT} = \frac{C_{AS} C_{AB}}{C_{AS}} \tag{2}$$

, and

$$C_{AT} = C_{AB}. \tag{3}$$

Volume can be represented,

$$V_{AS} = \rho_0 c^2 C_{AB} \tag{4}$$

where, ρ_0 is the density of air and c is the velocity of sound in air. Thus, the acoustic compliance and volume in the enclosure vary proportionally with each other. Note that the resonance frequency of the system, f_s, is determined by the acoustic compliance, C_{AT}. In other words, f_s could be a

function of the volume in the enclosure, V_{AS}, which eventually causes shifts in f_s (Figure S7c). In Figure S6c, the resonance frequency of the CBLSS without filling material is plotted as the internal volume is varied from 100 to 1,000 cc. Here, the relationship between f_s and V_{AS} can be represented in terms of an exponential function, as follows:

$$f_s = C_1 \exp(-V_B / C_2) + C_3 \tag{5}$$

where, V_B, C_1, C_2 and C_3 are the net internal volume of the enclosure and correlation coefficients, respectively. The correlation coefficients C_1, C_2 and C_3 are 133.35, 296.37 and 163.18, respectively. According to Small[2], V_{AS}, the volume of air, is equal to V_B, the net internal volume of the enclosure, when the enclosure contains only air under adiabatic conditions; i.e., there is no lining or filling material. However, if the enclosure does contain such materials, V_{AS}, which represents the acoustic compliance of the enclosure, is larger than V_B. If we modify Equation (5) in terms of internal volume, and measure f_S, the resonance frequency of the CBLSS, we can compute the effective volume V_{AB} in an enclosure with filling materials, as follows.

$$V_{AB} = C_2 \ln[(f_S - C_3) / C_1] \tag{6}$$

Hence, we can evaluate the effective volume-increasing effects of acoustic filling materials using Equation (6). Due to the shift in resonance frequency to lower frequency domains, we can improve the SPL in the low frequency region by modifying the conditions of the CBLSS enclosure using MF or adsorptive materials (Figure S7d).

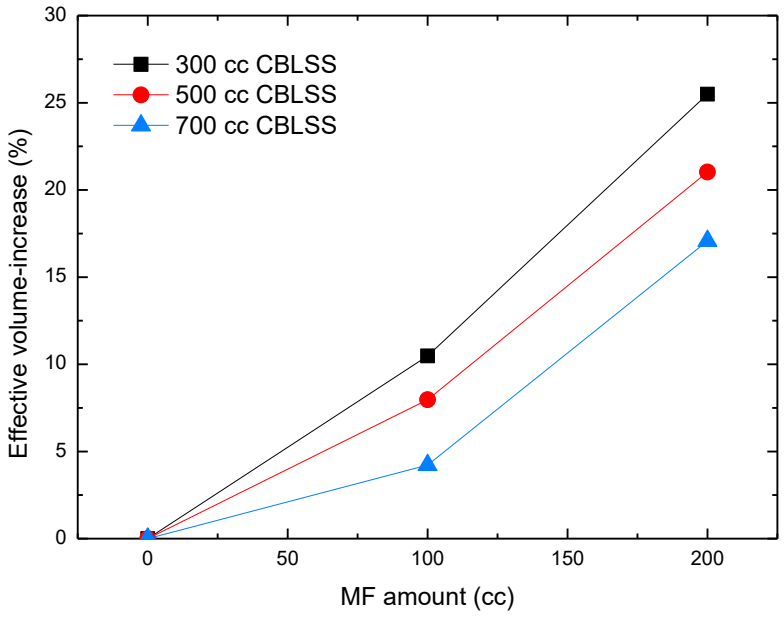

Figure S8. Effective volume-increasing effect of a square block of MF with respect to the amount in the CBLSS enclosure.

3. Acoustic analysis: measurement reliability

In this study, we putted all effort to meet repeatable condition. For instance, a single data is measured in same temperature (25 ℃), humidity and time slot (at night) in quiet environment. To check the validity of experimental data, representative data are measured in anechoic chamber and we checked the anechoic data and the data in lab have shown consistency each other. The measurement condition was 4 pi perfectly anechoic room ($7 \times 7 \times 7$ m^3) in SAMSUNG Electronics.

After we confirm the consistency in both data, we checked the data reliability in repeated tests (Figure S9).

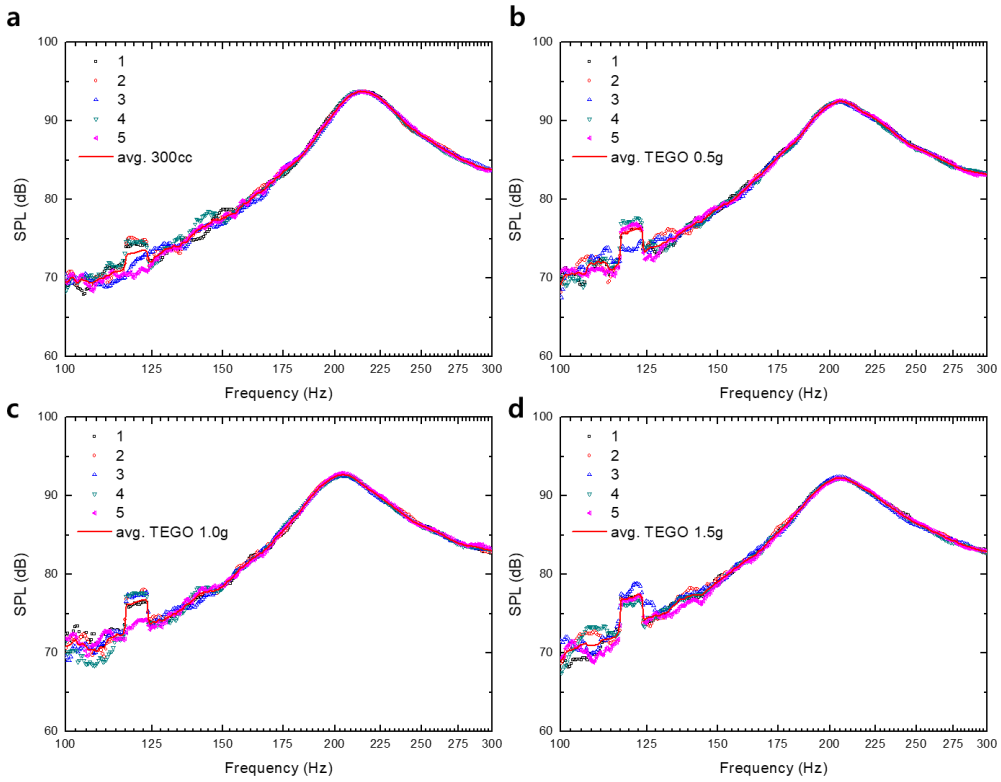

Figure S9. SPL of TEGO with different mass loading. (a) empty enclosure (300 cc). (b) TEGO 0.5g. (c) TEGO 1.0g. (d) TEGO 1.5g

As we discussed in previous chapter, we used acoustic analyzer (CLIO Pocket: Audiomatica). The measurement system works in frequency domain from 1 Hz to 45 kHz with 0.01 Hz of resolution. The acoustic analyzer generates a log chirp (sweeping signal) twice with 1/8 octave rate, and simultaneously measures the impedance or SPL at each frequency. For each case, we measured impedance and sound pressure level over five times and averaged them to get single curve as shown in Figure S10. The standard deviation of each case distributed up to 0.066 Ohm, but the optimum point of each impedance curve seems maintained. Accordingly, we are confident that the 6 Hz of change in single powder with different mass loading is meaningful value which is beyond the standard deviation.

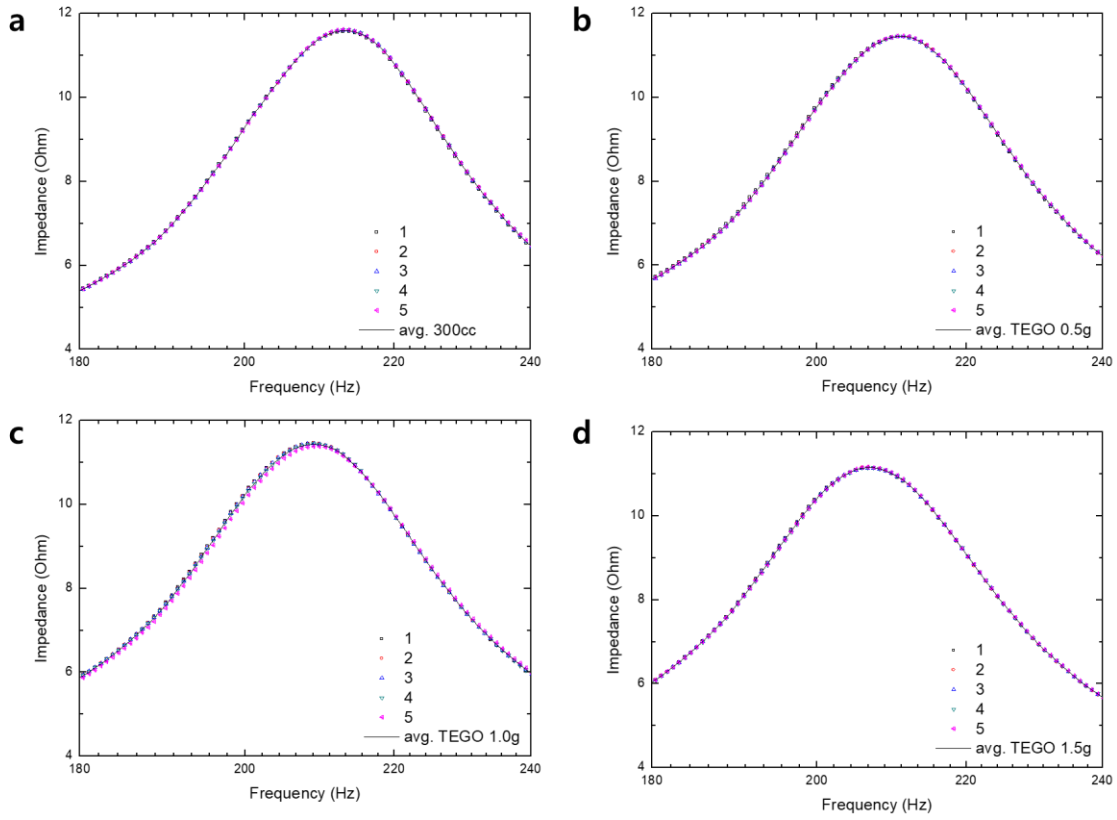

Figure S10. Raw data of the impedance curves for (a) 300cc of empty CBLSS, standard deviation = 0.025 ohm at 226.15 Hz; (b) TEGO 0.5g, standard deviation = 0.062 Ohm at 266.92 Hz; (c) TEGO 1.0g, standard deviation = 0.066 Ohm at 199.72 Hz; (d) TEGO 1.5g, standard deviation = 0.024 Ohm at 195.26 Hz.

Reference

(1) William, S.; Hummers, J.; Offeman, R. E. Preparation of Graphitic Oxide. *J. Am. Chem. Soc* **1958,** *80* (6), 1339-1339.

(2) Small, R. H. Closed-Box Loudspeaker Systems-Part 1: Analysis. *J. Aud. Eng. Soc.* **1972,** *20* (10), 798-808.

(3) Beranek, L. L.; Mellow, T. *Acoustics: Sound Fields and Transducers*, Academic Press: 2012.